


 CrossMark
click for updates

 Cite this: *Phys. Chem. Chem. Phys.*,
2015, 17, 7264

Electronic structure calculations of ESR parameters of melanin units

 Augusto Batagin-Neto,^{*a} Erika Soares Bronze-Uhle^b and
Carlos Frederico de Oliveira Graeff^b

Melanins represent an important class of natural pigments present in plants and animals that are currently considered to be promising materials for applications in optic and electronic devices. Despite their interesting properties, some of the basic features of melanins are not satisfactorily understood, including the origin of their intrinsic paramagnetism. A number of experiments have been performed to investigate the electron spin resonance (ESR) response of melanin derivatives, but until now, there has been no consensus regarding the real structure of the paramagnetic centers involved. In this work, we have employed electronic structure calculations to evaluate the ESR parameters of distinct melanin monomers and dimers in order to identify the possible structures associated with unpaired spins in this biopolymer. The *g*-factors and hyperfine constants of the cationic, anionic and radicalar structures were investigated. The results confirm the existence of at least two distinct paramagnetic centers in melanin structure, identifying the chemical species associated with them and their roles in electrical conductivity.

 Received 12th November 2014,
Accepted 10th February 2015

DOI: 10.1039/c4cp05256k

www.rsc.org/pccp

1 Introduction

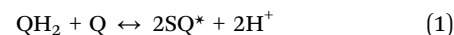
Melanins represent an important class of natural pigments found in plants and animals. In addition to this biopolymer's vital biological role, recent studies have pointed out melanins and their derivatives as interesting candidates for the construction of bioelectronic devices, highlighting their technological relevance.^{1–4}

Despite the promising opto-electronic properties of melanins, several of their basic features, such as their macromolecular structure, optical absorption, luminescence, conductivity and the origin of their intrinsic paramagnetism, are not satisfactorily understood.^{5,6} In particular, the presence of stable paramagnetic centers is widely reported in the literature.⁵ Such centers are detected experimentally through a persistent electron spin resonance (ESR) signal, which is detectable even under extreme experimental conditions.⁷ The observed responses are sensitive to external factors, such as pH,^{8,9} temperature,^{7,10} illumination,¹¹ the presence of oxidizing/reducing agents^{7,12,13} and metal centers,¹⁴ in such a way that a wide range of spectroscopic parameters are reported in the literature (*g*-factors, lineshapes and linewidths).

Much of what is currently known about the ESR spectra of melanins comes from studies of aqueous suspensions or dried

powders because these biomaterials are generally insoluble in several organic solvents.^{15,16} Regarding aqueous suspensions, it is observed that the signals are strongly influenced by the pH. At neutral and high pHs, an intense and relatively sharp ESR resonant line is observed. By reducing the pH of the solution, the ESR spectrum can be shifted to higher magnetic fields (or lower *g*-factors), along with signal broadening and intensity decrease, which is attributed to changes in the chemical balance of the paramagnetic centers present in the systems.^{8,9}

In general, the concentration of radicals in melanin solutions/suspensions is discussed in terms of the comproportionation equilibrium regarding the presence of fully reduced, fully oxidized and semi-reduced/oxidized monomeric units:



where QH₂ and Q represent *ortho*-hydroquinone and *ortho*-quinone, respectively, and SQ* represents semiquinone free radical units. The equilibrium is strongly shifted to the left in such a way that the concentration of radicals, SQ*, is quite low; typically, there is a ratio of 1 radical structure to 1000 completely oxidized or reduced structures.^{5,17} In basic solutions, the reaction is shifted towards the products, and in acidic samples, it is shifted towards the reactants.

Now, there is a consensus in the literature that melanin has two (or even more) paramagnetic centers that are detectable in both solid state and aqueous suspensions.^{8,9,18–20} One of these centers has a *g*-factor of around 2.003 and is mainly observed in acidic samples (or dried melanin powders^{7,20}), with no strong dependence of the spin density on pH and temperature.^{7,8}

^a Campus Experimental de Itapeva, UNESP - Univ Estadual Paulista, Rua Geraldo Alckmin 519, 18409-010, Itapeva, SP, Brazil. E-mail: abatagin@itapeva.unesp.br; Fax: +55 15 3524-9107; Tel: +55 15 3524-9100 ext. 9159

^b DF-FC, UNESP - Univ Estadual Paulista, Av. Eng. Luiz Edmundo Carrijo Coube 14-01, 17033-360 Bauri, SP, Brazil

A second center is observed in solutions with high pHs (or dried materials from basic or neutral samples²⁰), with a g -factor of around 2.005. The latter is strongly dependent on pH, presenting a higher spin density with higher sample basicity;^{8,9} a slight temperature dependence is also observed.¹⁰ Such low-field radicals ($g = 2.005$) have been associated with SQ* species from comproportionation reactions (eqn (1)),⁵ while high-field paramagnetic species ($g = 2.003$) are generally linked to intrinsic radicals present in the melanin structure.

Recently, Mostert *et al.*, in a study of melanin pellets, defined these two paramagnetic centers as semiquinone free radicals (SFR, with $g \sim 2.005$) and carbon-centered radicals (CCR, with $g \sim 2.003$).²⁰ By performing hydration-controlled experiments, they observed that the ESR spectrum of melanin in the solid state is dominated by CCR species⁷ and that very weak SFR signals could be observed in melanin pellets obtained from basic (and neutral pH) solutions. This weak component could be controlled by changing the pH of the precursor solutions, suggesting that the ESR spectrum of melanin in the solid state is also influenced by comproportionation reactions. They also observed a quenching of the CCR signals induced by water (or OH⁻) content, which was associated with destacking effects of melanin oligomers. Based on these statements, SFR centers were associated with SQ* species, while CCR signals were associated with paramagnetic centers located in the internal regions of the melanin macro-structure (protected from the environment).²⁰ Nevertheless, the structures associated with these centers were not discussed.

Following the denomination proposed by Mostert *et al.*, in contrast to the solid state, the ESR spectrum of melanin in aqueous solution is dominated by SFR signals, rather than CCR. However, at low pHs, as shown in the displacement of eqn (1) towards the reactants, CCR species begin to dominate the signal.

The g -values observed in melanins suggest that unpaired spins are located on a few units of these macromolecules, instead of being delocalized, which is reinforced by comparative studies of melanins, as well as by the related relaxation times.⁷ Such considerations suggest that relevant information about the ESR signal of melanins can be obtained by considering very small sub-units of this material.

In this sense, in order to identify the origin of the paramagnetic species responsible for the ESR signals of melanin, we compare the spin Hamiltonian parameters obtained from the electronic structure calculations for varied redox states of melanin monomers. Additional calculations involving dimeric units are also performed to evaluate the robustness of the results obtained. Finally, we attempt to correlate our findings with charge transport using the recently proposed ionic–electronic conductor model.^{1,3} The results provide important new insights regarding the nature of the paramagnetic centers observed in melanins, confirming the existence of two distinct ESR active groups in this material and pointing out the possible structures associated with them. Additionally, useful information is also provided regarding the charge transport mechanisms of melanin, which are important for the application of this material in bioelectronic devices.

2 Methodology

Fig. 1 shows the evaluated structures associated with distinct redox forms of DHI and DHICA melanin units.⁵ Anionic and cationic species were considered for HQ, IQ and QI structures. N-def and SQ structures were evaluated as radicals in their neutral state. The compound N-def was included to investigate the ESR response of possible synthesis sub-products.

In order to better evaluate the dependence of the ESR parameters on the position of the lateral groups, 50 distinct structures were constructed with randomly distributed OH and COOH dihedral angles for each species presented in Fig. 1. For IQ-DHI structures, dynamic molecular (DM) calculations were performed in order to obtain random structures. In this case, the DM simulation was performed by considering the molecule in contact with a reservoir at 1000 K during 1 ps (steps with 0.01 ps), following the methodology described in ref. 21. The Gabedit computational package was employed for this purpose.²²

The obtained geometries were pre-optimized *via* the PM6 semi-empirical method,²³ using an unrestricted Hartree–Fock (UHF) approach, and then fully optimized using DFT, employing Becke's LYP (B3LYP) exchange–correlation functional and the 6-31G basis set in an unrestricted Kohn–Sham (UKS) approach.

The ESR parameters were calculated after full optimization at the DFT level. Two distinct functionals, B3LYP and Perdew, Burke and Ernzerhof's hybridized functional (PBE0), were employed for comparison. 6-31G** and Barone's basis sets (EPRII)²⁴ were employed for the determination of g -factors and hyperfine constants, respectively. Such combinations of functionals and basis sets were employed because they usually provide high-quality ESR parameters for distinct systems.²⁵

The mean values of g -factors and hyperfine constants ($\langle X \rangle$) were evaluated by considering the probability of each structure's occurrence, as given by the Boltzmann factor (BF = $e^{-\Delta E_i/k_B T}$):

$$\langle X \rangle = \frac{\sum X_i e^{-\Delta E_i/k_B T}}{\sum e^{-\Delta E_i/k_B T}} \quad (2)$$

where X_i represents the value of the parameter X of the i -th structure (g -factor or isotropic hyperfine constant), ΔE_i represents the total energy difference between the i -th structure and the most stable one, k_B represents the Boltzmann's constant and T represents the temperature (considered equal to 300 K).

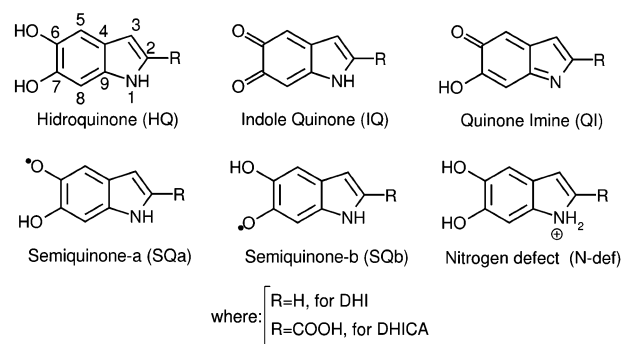


Fig. 1 Studied monomeric structures of melanin.

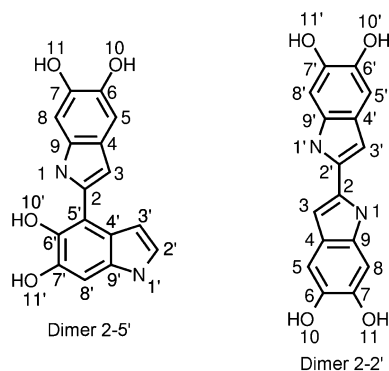


Fig. 2 Numbering used in the analysis of melanin dimers: 2–5' (left) and 2–2' (right).

In the dimer study, two distinct planar conformations were initially constructed and fully optimized in their neutral state. Fig. 2 shows the dimer's structures, as well as the atom labels employed in the analyses. Two distinct conformations were evaluated (identified by the numbers 01 and 02), which differed in the relative arrangement of the two monomeric units (rotation of 180° about the bonds 2–5' and 2–2').

Initial planar structures were considered for both dimers because preliminary optimization studies have indicated this configuration to be the most stable, which is in agreement with other theoretical studies.²⁶ The anionic and cationic structures were then fully optimized *in vacuo* in an UKS/B3LYP/6-31G approach, starting from previously optimized neutral structures. The g -factor values were evaluated *via* UKS/B3LYP/6-31G** and UKS/PBE0/6-31G** approaches.

The energy levels of the frontier orbitals (HOMO – highest occupied molecular orbital, LUMO – lowest unoccupied molecular orbital) were calculated by considering Koopmans' theorem ($E_{\text{HOMO}} = E_N - E_{N-1}$ and $E_{\text{LUMO}} = E_{N+1} - E_N$, where E_M represents the energy of the structure with M electrons).²⁷

The calculations were carried out with the GAMESS²⁸ (optimization) and ORCA²⁹ (ESR parameters) computer packages. The MOPAC2012 package^{30,31} was employed for the pre-optimizations.

3 Results and discussion

3.1 Monomers

Table 1 presents the mean g -factor values obtained from eqn (2) for the radical, anionic and cationic DHI and DHICA melanin monomers, using both B3LYP/6-31G** and PBE0/6-31G** approaches. As can be seen, quite similar results were obtained for the two functionals. In general, distinct redox species present dissimilar g -factors.

Fig. 3a–c illustrate the g -factor distribution of melanin monomers obtained from the B3LYP/6-31G** calculations. Similar results are obtained by using the PBE0/6-31G** approach. Boltzmann's factor, which is associated with the probability of the occurrence of each structure, is presented in the ordinate axes. The dotted lines represent the mean values presented in Table 1, which were obtained from eqn (2).

Table 1 Mean values of melanin monomer g -factors obtained from B3LYP/6-31G** and PBE0/6-31G** calculations

Structure	Species	B3LYP/6-31G**	PBE0/6-31G**
HQ-DHI	Anionic	2.00255	2.00257
	Cationic	2.00314	2.00314
HQ-DHICA	Anionic	2.00328	2.00332
	Cationic	2.00353	2.00352
IQ-DHI	Anionic	2.00567	2.00571
	Cationic	2.00544	2.00550
IQ-DHICA	Anionic	2.00563	2.00571
	Cationic	2.00554	2.00553
QI-DHI	Anionic	2.00451	2.00454
	Cationic	2.00328	2.00336
QI-DHICA	Anionic	2.00461	2.00466
	Cationic	2.00336	2.00338
N-def-DHI	Cation radical	2.00272	2.00273
N-def-DHICA	Cation radical	2.00317	2.00318
SQa-DHI	Free radical	2.00550	2.00558
SQa-DHICA	Free radical	2.00573	2.00581
SQb-DHI	Free radical	2.00519	2.00523
SQb-DHICA	Free radical	2.00564	2.00574

Note that small dispersions are observed around the mean values. The highest standard deviation is between 0.0003 and 0.0005 for SQ structures, suggesting that the g -factors are not very sensitive to the position of the lateral ligands of the monomers.

According to the mean values presented in Table 1 and Fig. 3a–c, it is possible to define two main groups:

- $g < 2.0040$:
 - radical structures: N-def-DHI e N-def-DHICA;
 - anionic structures: HQ-DHI e HQ-DHICA;
 - cationic structures: HQ-DHI, HQ-DHICA, QI-DHI e QI-DHICA.
- $g > 2.0040$:
 - radical structures: SQa-DHI, SQa-DHICA, SQb-DHI e SQb-DHICA;
 - anionic structures: IQ-DHI, IQ-DHICA, QI-DHI e QI-DHICA;
 - cationic structures: IQ-DHI e IQ-DHICA.

In particular, QI-DHI (anion) and QI-DHICA (anion) present intermediate g -values (~ 2.0045) as compared to the others.

The above-mentioned results reinforce the hypothesis that melanin's ESR signals are composed of at least two distinct paramagnetic centers. Indeed, the obtained values are compatible with carbon-centered radicals (CCR) and semiquinone free-radicals (SFR) signals, as proposed in ref. 20.

According to Mostert *et al.*, CCR has g -factors around 2.003, while SFR has g -factors between 2.0045 and 2.0050. Although our results reinforce this hypothesis, they also indicate that distinct structures are associated with each one of these centers. The g -values obtained for SQ species are indeed compatible with SFR signals. However, IQ-anion, IQ-cation and QI-anion species also have g -factors close to 2.005, indicating that they could also be associated with SFR centers. On the other hand, both the HQ charged species, as well as the N-def and QI-cation structures, present g -factors that are compatible with CCR signals.

Fig. 4 presents an estimation of the electron affinity (E_A) and ionization potential (IP) associated with each of the neutral monomeric species presented in Fig. 1 (obtained from

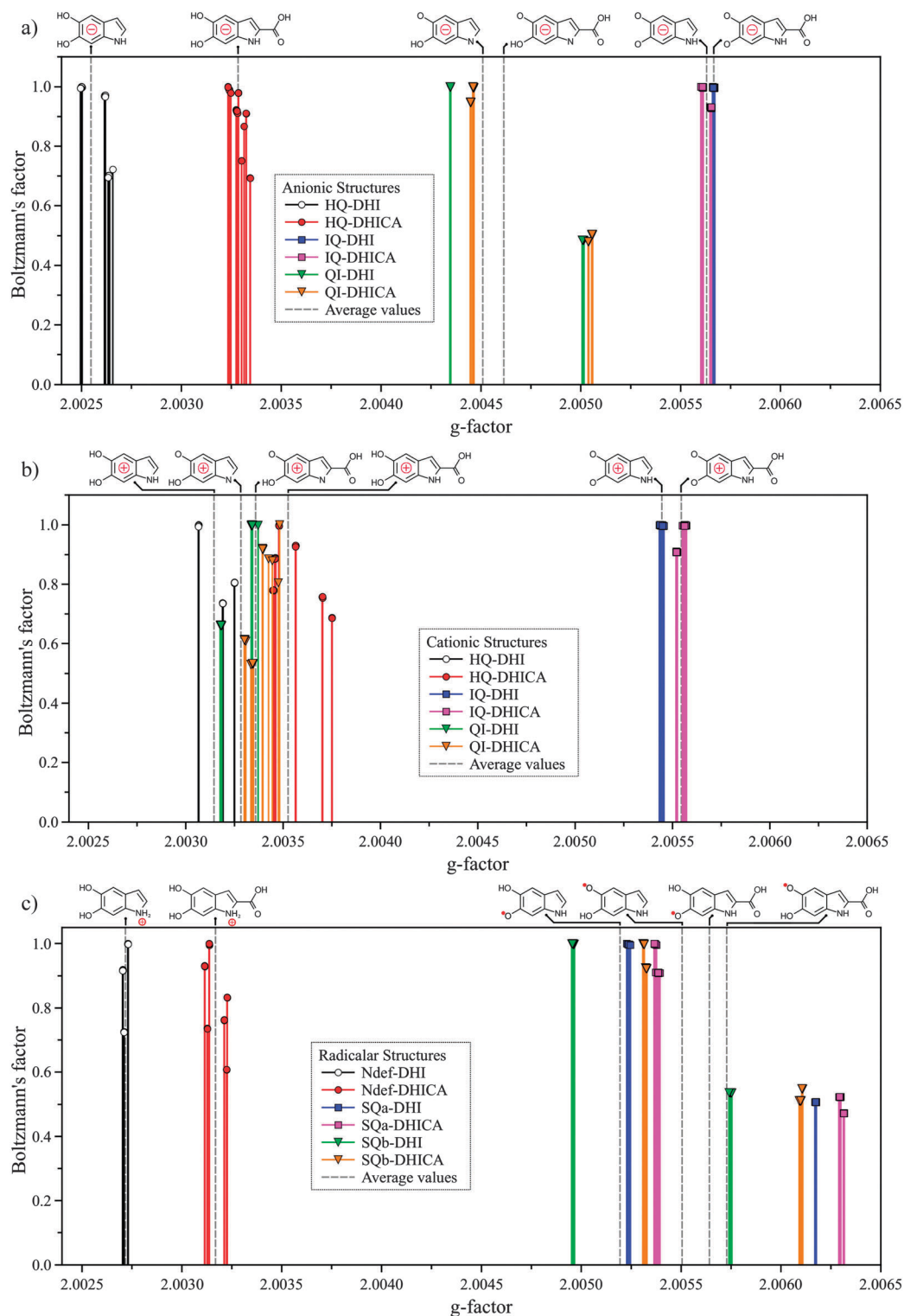


Fig. 3 Distribution of melanin monomer g -factors obtained from the B3LYP/6-31G** approach: (a) anionic, (b) cationic and (c) radical structures. Dotted lines indicate the mean values obtained from eqn (2).

$IP = E(N - 1) - E(N)$ and $E_A = E(N) - E(N + 1)$,²⁷ where $E(M)$ represents the total energy of monomeric species with M electrons).

All structures present IP values higher than 0.25 eV and absolute E_A values lower than 0.10 eV. In particular, negative E_A

values are observed for HQ structures, indicating that the incorporation of one electron into these monomers is accompanied by an increase in their energy. This result, however, does not mean that HQ-anion species cannot be encountered in

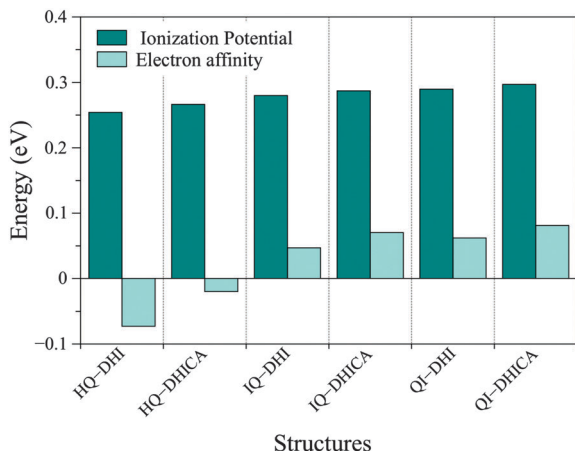


Fig. 4 Electron affinity and ionization potential of HQ, IQ and QI monomeric structures of melanin.

a melanin macro-structure. It only suggests that HQ-anions are less probable than other anionic structures. In fact, distinct IP and E_A values are expected in extended oligomers (dimers, trimers, tetramers, *etc.*).^{5,32} Thus, the values presented in Fig. 4 merely show a trend. For example, we can observe that the absolute IP values are, in general, higher than the E_A values, indicating that anionic monomers are more easily generated *via* simple electron transfer than cations. This result suggests that negatively charged species are more likely than cationic structures to be associated with the melanin's ESR signal. In this context, given the g -values obtained for the charged structures, HQ-anions are promising candidates for CCR species, while IQ-anions and QI-anions can be linked to SFR signals. Nevertheless, it is also important to keep in mind that protonation processes can also take place in these systems. Thus, cationic and N-def species could also be generated from the attachment of H^+ onto the structures with unprotected lateral oxygens (such as IQ, QI and SQ) or onto the nitrogen of the HQ structures.

Let us focus on the paramagnetic centers observed experimentally in melanin derivatives. The g -factors from our calculations suggest that N-def, HQ-anion, HQ-cation and QI-cation can be associated with CCR signals. In general, the ESR signal of melanin in aqueous solutions is dominated by SFR species. However, by reducing the pH, a shift in the spectra towards higher magnetic fields (lower g -factors) is observed, which can be attributed to the CCR signal. In this case, the presence of H^+ ions in the system could be responsible for the annihilation of the competing SFR species (a shift in the comproportionation reaction toward reactants), followed by two distinct effects: (i) the stabilization of negatively charged subunits of melanin located in internal regions of the macromolecules, suggesting the relevance of HQ-anionic structures, or (ii) the protonation of the monomeric units located at the interface of melanin's macro-structure and the solvent, leading to the formation of protonated species, such as HQ-cation and N-def. Because unprotected oxygens are present in the structure of QI-cation, the protonation process cannot explain the generation of such

species in the system, thus eliminating this structure as an active CCR component.

In spite of its plausibility, the hypothesis associated with the protonation of melanin units at the interface is unlikely. Experimentally, the spin density shows no dependence on pH in acidic solutions. In other words, the concentration of spins is approximately constant for pHs below 7.⁸ This observation suggests that an increased concentration of H^+ ions in the systems does not induce the formation of new ESR active centers, discrediting the sub-unit protonation hypothesis. Apparently, at a low pH, the SFR species are consumed by comproportionation reactions (eqn (1)), while CCR paramagnetic centers, which were already present in the system, are not affected and begin to dominate the spectrum.

These considerations suggest that CCR signals can be associated with anionic HQ units located in the internal regions of melanin's macro-structure. N-def species created by the incomplete cyclization of L-DOPA (instead of protonation reactions) could also be considered as another possible CCR structure. Both of these species must be located in the internal regions of the melanin macro-structure and thus be protected from the action of chemical species from the solvent, such as OH^- groups and protons, which is in good agreement with the work of Mostert *et al.*²⁰

Indeed, this proposal is compatible with the temperature dependence of the melanin ESR signal in solid-state and aqueous suspensions.^{7,10} Because CCR species are protected from the environment, the influence of temperature should be weak, so the ESR signal of dried material shows a Curie dependence on T (signal proportional to T^{-1}).⁷

In relation to the SFR paramagnetic centers, our results suggest that the SQ, IQ-anion, IQ-cation and QI-anion structures are possible ESR active species. Because SFR species dominate the ESR signal in high pHs, it is very unlikely that IQ-cation structures contribute. This structure shows a high PI value and cannot be obtained *via* protonation processes in basic solutions. In this sense, the SFR paramagnetic centers must be mainly associated with IQ-anion, QI-anion and SQ radicals. Indeed, similar structures associated with all of these species could be generated from H^+ abstraction. Additionally, it is known that SFR signals are more sensitive to temperature than CCR, which suggests that their concentration depends on the reaction rates among chemical species present in the solvent and the sub-units of melanin located at the macro-structure surface.¹⁰

In order to better evaluate the expected spectroscopic characteristics of each of the proposed structures, the hyperfine coupling constants were calculated. Tables 2 and 3 show the average values of the isotropic hyperfine constant, A_{iso} , obtained *via* the B3LYP/EPRII approach (through eqn (2)). Fig. 5 shows the atom numbering adopted for hydrogen and nitrogen atoms in both the DHI and DHICA monomers. Similar results were obtained by using PBE0/EPRII.

In general, DHICA monomers (Table 3) show less intense hyperfine interactions than DHI (Table 2), suggesting the existence of an increased spin delocalization on these compounds. This effect is probably induced by the presence of the carboxylic

Table 2 Mean values of the hyperfine coupling constants obtained via DFT/B3LYP/EPRII for the hydrogen and nitrogen atoms of DHI monomeric structures

Atom number (Fig. 5)	A_{iso} (mT)								
	HQ-DHI		IQ-DHI		QI-DHI		N-def-DHI	SQa-DHI	SQb-DHI
	Anion	Cation	Anion	Cation	Anion	Cation			
1	0.019	0.122	0.124	0.390	0.064	0.294	0.316	0.019	0.073
2a	0.054	0.078	0.031	0.607	—	—	2.455	0.110	0.028
2b	—	—	—	—	—	—	2.622	—	—
3	0.564	0.729	0.427	0.080	0.336	0.042	0.265	0.074	0.624
4	0.028	0.133	0.054	0.708	0.052	1.182	0.728	0.092	0.142
5	0.353	0.072	0.341	1.044	0.329	0.364	0.316	0.617	0.216
6	0.400	0.220	—	—	—	—	0.003	—	—
7	1.644	0.342	—	—	0.083	0.262	0.063	0.132	0.138
8	0.256	0.086	0.166	0.675	0.051	0.274	0.169	0.193	0.544
Average	0.415	0.223	0.190	0.584	0.153	0.403	0.771	0.177	0.252

Table 3 Mean values of the hyperfine coupling constants obtained via DFT/B3LYP/EPRII for the hydrogen and nitrogen atoms of DHICA monomeric structures

Atom number (Fig. 5)	A_{iso} (mT)								
	HQ-DHICA		IQ-DHICA		QI-DHICA		N-def-DHICA	SQa-DHICA	SQb-DHICA
	Anion	Cation	Anion	Cation	Anion	Cation			
1	0.086	0.094	0.101	0.417	0.080	0.291	0.162	0.017	0.024
2a	0.180	0.163	0.044	0.647	—	—	1.510	0.094	0.077
2b	—	—	—	—	—	—	1.511	—	—
3	0.091	0.024	0.041	0.010	0.015	0.026	0.075	0.005	0.040
4	0.519	0.062	0.154	0.641	0.313	1.135	1.072	0.198	0.226
5	0.471	0.080	0.562	0.959	0.574	0.328	0.351	0.755	0.223
6	0.009	0.341	—	—	—	—	0.006	—	—
7	0.333	0.269	—	—	0.043	0.276	0.071	0.106	0.128
8	0.172	0.065	0.089	0.799	0.021	0.292	0.150	0.176	0.639
Average	0.233	0.137	0.165	0.579	0.174	0.391	0.546	0.193	0.194

group, which is responsible for the withdrawal of electrons from the rings.

Another interesting feature regarding the CCR and SFR signals is the difference observed in the ESR spectral linewidth at low (CCR-dominated) and high (SFR-dominated) pHs. It is experimentally observed that basic samples show signals with higher linewidths than acidic samples ($\Delta H_{1/2}$),⁸ which suggests, among other factors, the existence of stronger (and/or more unresolved) hyperfine couplings in CCR species than in SFR species.

In this context, the relatively high values of A_{iso} associated with HQ-anion and N-def species (with respect to SQs) reinforce the hypothesis that these structures can be assigned to the CCR signal. In particular, the higher hyperfine constants observed in these monomers are not associated with the common polymerization sites of melanins (sites 2, 5 and 8, as presented in Fig. 1), so they should be observed in larger structures (dimers, trimers, *etc.*). SQ, IQ-anion and QI-anion species, on the other hand, show smaller hyperfine constants, which are also compatible with SFR signals with smaller linewidths. Additionally, the highest A_{iso} values of these structures are linked to sites 2, 5 or 8, which are typical polymerization sites for melanin, so even lower hyperfine couplings are expected for these structures in fully polymerized material. The same trends are observed for DHI and DHICA derivatives, with a greater dispersion of the hyperfine contribution for DHICA.

Another piece of relevant information is that the mean A_{iso} values of HQ cationic species are generally lower than those related to SQs, suggesting once more that HQ-cation species are not associated with CCR signals. However, it is also important to keep in mind that the larger linewidths observed in the CCR signal could also be associated with the co-existence of ESR active species with distinct g -factors (g -strain effect) that cannot be explained by the structural features of the monomers (low dispersion of the g -factors, as shown in Fig. 1), so the existence of other species in the systems, like HQ-cations, cannot be totally discarded.

In summary, both the analyses involving g -factors and hyperfine constants indicate that SFR signals are mainly associated with SQ, IQ-anion and QI-anion species, whereas CCR signals are mostly related to HQ-anion and N-def species located in internal regions of the melanin macro-structure.

3.2 Dimers

In order to investigate whether the trends obtained for melanin monomers will also be observed for larger structures, we evaluated the g -factors of two melanin dimers commonly reported in the literature.^{33,34} Such structures were also identified as the most likely dimeric structures based on monomer reactivity studies (to be published). The structures evaluated are presented in Fig. 2.

Tables 4 and 5 show the results obtained for dimers 2–5' and 2–2' in conformations 01 and 02 using different functionals.

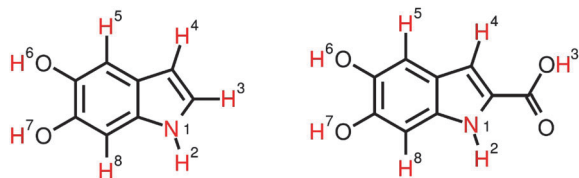


Fig. 5 Labels adopted for hydrogen and nitrogen atoms for the study of hyperfine constants: DHI (left) and DHICA (right) monomeric structures.

Table 4 g -factor obtained for different structures of the 2–5' dimer via B3LYP/6-31G** and PBE0/6-31G**

Dimers 2–5'	Species	Conformer 01		Conformer 02	
		B3LYP	PBE0	B3LYP	PBE0
HQHQ	Anionic	2.00274	2.00275	2.00274	2.00276
	Cationic	2.00297	2.00296	2.00296	2.00295
IQIQ	Anionic	2.00545	2.00557	2.00532	2.00539
	Cationic	2.00511	2.00511	2.00527	2.00526
QIQI	Anion	2.00479	2.00496	2.00454	2.00470
	Cationic	2.00293	2.00291	2.00293	2.00289
SQSQ	Anionic	2.00572	2.00572	2.00620	2.00620
	Cationic	2.00555	2.00562	2.00570	2.00598
HQIQ	Anionic	2.00532	2.00537	2.00537	2.00542
	Cationic	2.00381	2.00388	2.00370	2.00380
IQHQ	Anionic	2.00547	2.00557	2.00529	2.00539
	Cationic	2.00489	2.00487	—	—
HQQI	Anionic	2.00457	2.00463	2.00426	2.00430
	Cationic	2.00329	2.00329	2.00347	2.00344
QIHQ	Anionic	2.00509	2.00516	2.00500	2.00507
	Cationic	2.00323	2.00330	2.00342	2.00351
IQQI	Anionic	2.00483	2.00496	2.00447	2.00455
	Cationic	2.00458	2.00448	2.00507	2.00503
QIIQ	Anionic	2.00537	2.00553	2.00496	2.00509
	Cationic	2.00361	2.00377	2.00368	2.00383
HQSQ	Free radical	2.00488	2.00497	2.00461	2.00468
SQHQ	Free radical	2.00625	2.00636	2.00618	2.00629
IQSQ	Free radical	2.00529	2.00540	2.00516	2.00523
SQIQ	Free radical	—	—	2.00647	2.00672
QISQ	Free radical	2.00496	2.00517	2.00515	2.00539
SQQI	Free radical	2.00633	2.00646	2.00620	2.00637

Table 5 g -factor obtained for different structures of the 2–2' dimer via B3LYP/6-31G** and PBE0/6-31G**

Dimers 2–2'	Species	Conformer 01		Conformer 02	
		B3LYP	PBE0	B3LYP	PBE0
HQHQ	Anionic	2.00276	2.00278	2.00275	2.00277
	Cationic	2.00304	2.00303	2.00296	2.00294
IQIQ	Anionic	2.00593	2.00610	2.00608	2.00625
	Cationic	2.00571	2.00531	2.00532	2.00507
QIQI	Anionic	2.00469	2.00484	2.00467	2.00481
	Cationic	2.00290	2.00287	2.00294	2.00288
SQSQ	Anionic	2.00556	2.00558	2.00562	2.00563
	Cationic	2.00831	2.00885	2.00852	2.00904
HQIQ	Anionic	2.00551	2.00560	2.00555	2.00565
	Cationic	2.00484	2.00472	2.00476	2.00465
HQQI	Anionic	2.00514	2.00522	2.00525	2.00534
	Cationic	2.00350	2.00355	2.00352	2.00357
IQQI	Anionic	2.00551	2.00566	2.00545	2.00554
	Cationic	2.00461	2.00443	—	—
HQSQ	Free radical	2.00633	2.00645	2.00641	2.00653
IQSQ	Free radical	2.00656	2.00668	2.00660	2.00672
QISQ	Free radical	2.00739	2.00755	2.00768	2.00777

Fig. 6 illustrates the g -factor distribution of the dimers for B3LYP/6-31G** (average values taken from conformations 01 and 02). The g -factor calculations were not performed for structures 2–5'/IQHQ-02, 2–5'/SQIQ-01 and 2–2'/IQQI-02, because it was not possible to obtain stable structures for these conformations. However, as can be seen from the analysis of other dimers, a good estimate of the parameters for these structures can be obtained *via* their conformers.

In fact, very similar results are obtained for the 01 and 02 conformations for all dimers and in both approaches. First, let us analyze the dimers composed of two equal units, which are referred to here as “homo-structured dimers”: HQHQ, IQIQ, QIQI and SQSQ. In all these structures, essentially, we observe the same g -factors already obtained for the monomeric units in the 2–2' and 2–5' dimers. Variations are observed for the SQSQ-cation structures.

Regarding “hetero-structured” dimers, the sequence that determines the influence of the monomeric units in the dimer's g -factor is as follows: HQ < QI < IQ. Anomalous behavior is observed for SQ-based dimers, for which we have observed higher g -factor values than those obtained for SQ monomers. In general, the g -factor of anionic dimers is dominated by species that present unprotected lateral oxygens (O-unprotected structures); this trend is observed for both the 2–2' and 2–5' dimers. In the case of cationic structures, the IQ and HQ units have a greater influence, so intermediate g -factors (in relation to the monomeric building blocks) are obtained for HQIQ (IQHQ), HQQI (QIHQ) and IQQI (QIIQ) structures. For the 2–5' dimer in particular, it can be observed that the monomeric unit connected through site 2 (represented in the vertical position in Fig. 2) has a greater influence in the g -factors of the dimers than the unit connected through site 5' (represented in the horizontal position in Fig. 2). The greater influence of O-unprotected structures in the g -factor of the hetero-structured dimers indicates that the ESR signal of melanins is dominated by SFR species (IQ-anion, QI-anion and SQ species), which is indeed compatible with the experimental results.

Notice, from Tables 4 and 5, that the attachment of SQ monomers to all the other units results in dimeric species with g -factors higher than 2.006, suggesting the presence of more confined paramagnetic centers in these structures than would be predicted for SQ monomers. This result indicates that SQ species may not be directly linked to SFR signals ($g = 2.005$). In this context, IQ-anion and QI-anion are more plausible candidates because the g -values of dimers containing these units have not shown significant changes in relation to the monomers, still being compatible with the SFR signal. Indeed, more recent versions of comproportionation reactions indicate that IQ-anion occupies the place of the SQ* units in eqn (1), which is in good agreement with our results.^{1,20}

In summary, the results suggest that the main features of the ESR spectrum of melanin can be interpreted in terms of sub-units of this material, reinforcing the hypothesis that the unpaired electrons, which are responsible for the ESR signals, are indeed located on just a few molecular units.⁷

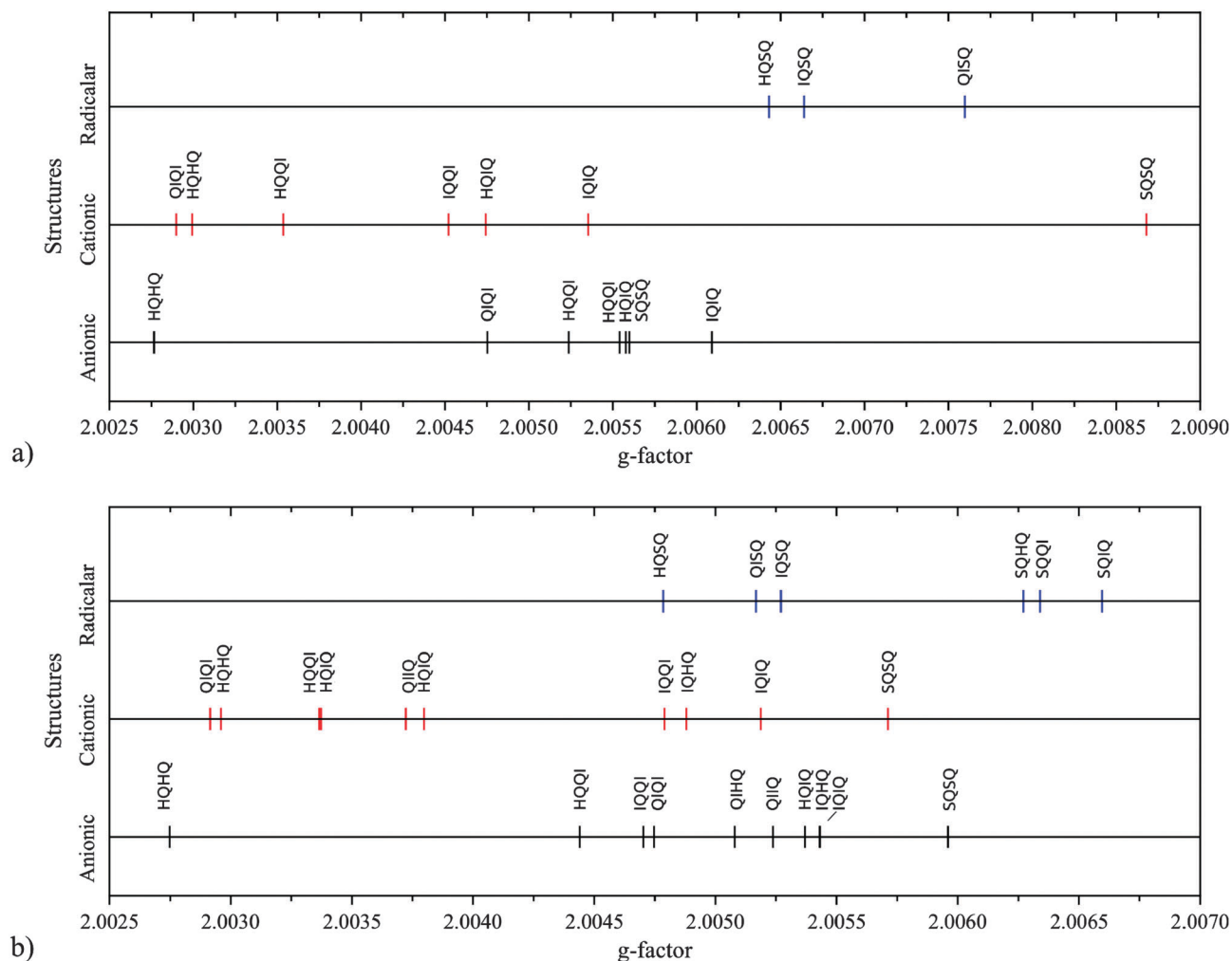


Fig. 6 g-factor distribution of melanin dimers obtained from the B3LYP/6-31G** approach (average values obtained from structures 01 and 02): (a) dimer 2-2' and (b) dimer 2-5'.

3.3 Considerations regarding charge carriers in melanin

Since the 1970s, the electrical and optical properties of melanins have been explained by considering them to be natural amorphous semiconductors.^{3,35} In this context, the widely reported dependence of the electrical conductivity of melanins on the hydration level of the samples has been interpreted in terms of the Mott-Davis amorphous semiconductor model (MDAS).³ Such an interpretation, however, was controversial because the observed dependence was so strong that no electrical conductivity could be observed in fully dried samples.³⁶

Recently, *via* the hydration-controlled electrical characterization of melanin-based devices, Mostert and collaborators have demonstrated that the response of wet samples is not compatible with MDAS predictions.^{1,37} By using muon spin relaxation and electron paramagnetic resonance measurements, they suggested that melanin behaves like a hybrid ionic-electronic conductor. In this context, it was proposed that the hydration level of the samples can perturb the comproportionation equilibrium in the solid state in such a way

that eqn (1) is shifted toward the products for hydrated samples, providing protons and electrons for conduction (self-doping mechanisms). Mostert *et al.* also demonstrated that CCR species could not be directly linked to melanin conductivity, suggesting that SFR units dominate the electronic transport of the material.

In the context of the present work, such information suggests that SFR species act as sources of electrons for conduction, while CCR species act as electron (or hole) traps in the samples. The study of charge transport in melanins is not within the scope of this paper. However, we believe that simple energy level analysis could provide some relevant clues to outline the nature of the charge carriers present in the material and then bring additional information regarding CCR and SFR species to light.

Fig. 7 shows the energy levels of frontier orbitals associated with melanin monomers: the highest occupied molecular orbital (HOMO), the lowest unoccupied molecular orbital (LUMO) and the singly occupied molecular orbital (SOMO – for radicalar structures*).

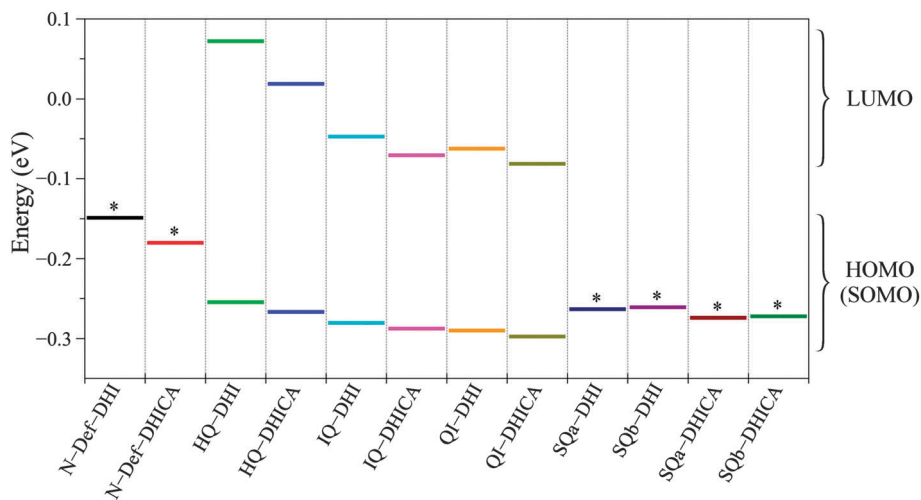


Fig. 7 Energy level alignments of frontier orbitals of melanin monomers: (i) the lowest unoccupied molecular orbital (LUMO), (ii) the highest occupied molecular orbital (HOMO) and (iii) the singly occupied molecular orbital (SOMO) for radical structures (*).

Let us first evaluate the CCR species. In Sections 3.1 and 3.2, we have proposed that CCR species could be associated with HQ-anion and N-def structures, both of which are present in the internal regions of melanin macromolecules. However, given the energy level alignments presented in Fig. 7 and the interpretation of melanin's conductivity proposed in ref. 1, we can conclude that N-def structures are more appropriate candidates. N-def should act as an electron/hole trap in melanin macromolecules (with a difference in energy between $3.5kT$ and $5.9kT$ for HQ units and even higher for the other units), which is in agreement with the findings of Mostert *et al.*¹ On the other hand, if CCR centers were linked to HQ-anions, a significant contribution should be expected from these species in the electrical conductivity of melanins, which was not observed.

However, the interpretation regarding SFR is not so direct. According to Fig. 7, if SQ units were generated *via* a comproportionation reaction, the conductivity of melanins should be dominated by holes. On the other hand, if IQ-anion and QI-anion structures were formed, the conductivity should be dominated by electrons.

In the case of SQ formation, given the high level of alignment observed among all the units, efficient hole transport is expected to occur in bulk melanin. Because no energetic barriers are present in the material, SFR formation should be followed by hole diffusion to bulk melanin and strong CCR annihilation *via* hole capture in N-def defects, which is not compatible with the experimental results. Indeed, only very weak consumption of CCR centers is observed after melanin hydration (which has been attributed to melanin destacking effects).²⁰ Additionally, if melanin electronic transport was dominated by SQ units, a very high electronic conductivity should be expected for this material, which is not observed (except at the "on" state of the melanin threshold switch).

In the case of IQ-anion or QI-anion formation, on the other hand, electron-dominated transport is expected to be hindered by internal HQ units (acting as energetic barriers to the charge carrier),

turning the transport of electrons in the bulk into a more difficult task than that related to the holes (material with lower conductivity). In addition, the consumption of CCR species by electrons is not expected to be an efficient process, because it should be limited by the higher energetic disorder of the material for electron transport, which is more compatible with the experimental results.

An additional feature that must be stressed in the case of charge transport dominated by IQ-anion/QI-anion is that the electron transport should occur preferentially by hopping between $IQ^-/QI^- \rightarrow IQ^0/QI^0$ and $IQ^-/QI^- \rightarrow IQ^-/QI^-$ species (M^0 : neutral structures), where the last defines a spin-dependent process involving the formation of dianions.³⁸ Because SFR species are expected to be formed mainly on the surface of melanin macromolecules (the interface between melanin and water molecules), such transport should essentially occur through pathways on the material surface, and then, it must be very sensitive to electron spin resonance techniques, suggesting that new electrical characterization tools could be employed to evaluate the charge transport of melanins.

Still, in this context, another relevant feature favoring the association of IQ-anion and QI-anion with SFR species is the threshold switch phenomena observed in melanins. As reported by McGinness *et al.*,³⁵ the intense electrical current obtained at the "on" state of melanin-based devices could not be associated only with the ionic conduction of water molecules, suggesting the existence of additional charge transport processes (probably associated with an electronic component due to SFR species formation). By considering the consumption of HQ units *via* comproportionation reactions (possibility intensified by local pH gradients³⁹), the generation of IQ-anion and QI-anion species on the surface of melanin's macromolecules could establish a very efficient percolative electron pathway, which could be partially responsible for the observed threshold switch.

4 Conclusions

ESR parameters, such as g -factors and hyperfine interaction constants, were evaluated for various monomers and dimers of melanin *via* electronic structure calculations, using a DFT approach. Anionic, cationic and radical structures were evaluated.

A reasonable number of initial structures were considered in the optimizations, and a wide dispersion of the parameters was observed. The results obtained confirm the presence of at least two groups of structures with different g -factors, which have already being experimentally observed and classified as carbon-centered radicals (CCR) and semiquinone free radicals (SFR). Based on the g -factors and hyperfine constants obtained for the monomeric units, we associate CCR species with HQ-anion and N-def structures and SFR species with SQ, IQ-anion and QI-anion structures.

The g -factors of dimeric oligomers suggest that the ESR spectrum of larger structures may be interpreted in terms of the parameters obtained from the monomers. In general, we have noted that the spectra of larger structures are dominated by species with unprotected oxygens. The following order of dominance is observed: HQ < IQ < QI. Dimers based on SQ species showed very high g -factors, suggesting that these species are not directly related to the SFR signal, contrary to what is normally suggested in the literature.

Simple analyses involving the energy levels of the monomers and charge transport processes suggest that CCR species are more compatible with N-def structures than HQ-anion structures. In turn, SFR species are more associated with QI-anion and IQ-anion structures than SQ structures. Such results provide relevant information regarding the nature of melanin charge carriers, suggesting that charge transport in these materials can also be accompanied by spin-dependent processes.

Acknowledgements

The authors would like to acknowledge the Fundação de Amparo à Pesquisa do Estado de São Paulo (FAPESP) (Proc. 2012/03116-7) and Instituto Nacional de Ciências dos Materiais em Nanotecnologia (INCTMN) (08/57872-1) for their financial support. This research was also supported by resources supplied by the Center for Scientific Computing (NCC/GridUNESP) of São Paulo State University (UNESP).

References

- 1 A. B. Mostert, B. J. Powell, F. L. Pratt, G. R. Hanson, T. Sarna, I. R. Gentle and P. Meredith, *Proc. Natl. Acad. Sci. U. S. A.*, 2012, **109**, 8943–8947.
- 2 J. Wünsche, L. Cardenas, F. Rosei, F. Cicoira, R. Gauvin, C. F. O. Graeff, S. Poulin, A. Pezzella and C. Santato, *Adv. Funct. Mater.*, 2013, **23**, 5569.
- 3 P. Meredith, K. Tandy and A. B. Mostert, in *Org. Electron.*, ed. F. Cicoira and C. Santato, Wiley-VCH Verlag GmbH & Co. KGaA, 2013, pp. 91–111.
- 4 M. Piacenti da Silva, J. C. Fernandes, N. B. de Figueiredo, M. Congiu, M. Mulato and C. F. O. Graeff, *AIP Adv.*, 2014, **4**, 037120.
- 5 P. Meredith and T. Sarna, *Pigm. Cell Res.*, 2006, **19**, 572–594.
- 6 P. Meredith, B. J. Powell, J. Riesz, S. P. Nighswander-Rempel, M. R. Pederson and E. G. Moore, *Soft Matter*, 2006, **2**, 37.
- 7 M. S. Blois, A. B. Zahlan and J. E. Maling, *Biophys. J.*, 1964, **4**, 471–490.
- 8 S.-S. Chio, J. S. Hyde and R. C. Sealy, *Arch. Biochem. Biophys.*, 1982, **215**, 100–106.
- 9 M. Pasenkiewicz-Gierula and R. C. Sealy, *Biochim. Biophys. Acta*, 1986, **884**, 510–516.
- 10 S.-S. Chio, J. S. Hyde and R. C. Sealy, *Arch. Biochem. Biophys.*, 1980, **199**, 133–139.
- 11 T. Sarna and R. Sealy, *Arch. Biochem. Biophys.*, 1984, **232**, 574–578.
- 12 R. Dunford, E. J. Land, M. Rozanowska, T. Sarna and T. Truscott, *Free Radicals Biol. Med.*, 1995, **19**, 735–740.
- 13 K. J. Reszka, Z. Matuszak and C. F. Chignell, *Free Radicals Biol. Med.*, 1998, **25**, 208–216.
- 14 L. Najder-Kozdrowska, B. Pilawa, A. B. Wickowski, E. Buszman and D. Wrzeniok, *Appl. Magn. Reson.*, 2009, **36**, 81–88.
- 15 G. Prota, *Melanins and Melanogenesis*, Academic Press, 1st edn, 1992.
- 16 E. S. Bronze-Uhle, A. Batagin-Neto, P. H. Xavier, N. I. Fernandes, E. R. de Azevedo and C. F. Graeff, *J. Mol. Struct.*, 2013, **1047**, 102–108.
- 17 W. Froncisz, T. Sarna and J. S. Hyde, *Arch. Biochem. Biophys.*, 1980, **202**, 289–303.
- 18 F. J. Grady and D. C. Borg, *J. Am. Chem. Soc.*, 1968, **90**, 2949–2952.
- 19 M. d'Ischia, A. Napolitano, A. Pezzella, P. Meredith and T. Sarna, *Angew. Chem., Int. Ed.*, 2009, **48**, 3914–3921.
- 20 A. B. Mostert, G. R. Hanson, T. Sarna, I. R. Gentle, B. J. Powell and P. Meredith, *J. Phys. Chem. B*, 2013, **117**, 4965–4972.
- 21 A. Batagin-Neto, E. F. Oliveira, C. F. Graeff and F. C. Lavarda, *Mol. Simul.*, 2013, **39**, 309–321.
- 22 A.-R. Allouche, *J. Comput. Chem.*, 2011, **32**, 174–182.
- 23 J. J. P. Stewart, *J. Mol. Model.*, 2007, **13**, 1173–1213.
- 24 V. Barone, *Recent Advances in Density Functional Methods*, World Scientific, 1995, vol. 1, pp. 287–334.
- 25 F. Neese, *High resolution EPR: applications to metalloenzymes and metals in medicine*, Springer, Nova York, EUA, 2009, vol. 28.
- 26 K. B. Stark, J. M. Gallas, G. W. Zajac, M. Eisner and J. T. Golab, *J. Phys. Chem. B*, 2003, **107**, 3061–3067.
- 27 E. G. Lewars, *Computational Chemistry: Introduction to the Theory and Applications of Molecular and Quantum Mechanics*, 2nd edn, Springer, 2010.
- 28 M. W. Schmidt, K. K. Baldridge, J. A. Boatz, S. T. Elbert, M. S. Gordon, J. H. Jensen, S. Koseki, N. Matsunaga, K. A. Nguyen, S. Su, T. L. Windus, M. Dupuis and J. A. Montgomery, *J. Comput. Chem.*, 1993, **14**, 1347–1363.
- 29 F. Neese, *Wiley Interdiscip. Rev.: Comput. Mol. Sci.*, 2012, **2**, 73–78.

- 30 J. J. P. Stewart, *J. Comput.-Aided Mol. Des.*, 1990, **4**, 1–103.
- 31 J. J. P. Stewart, *MOPAC2012: Molecular Orbital Package*, 2012.
- 32 T. Sarna and H. A. Swartz, in *The Pigmentary System*, ed. J. J. Nordlund, R. E. Boissy, V. J. Hearing, R. A. King, W. S. Oetting and J.-P. Ortonne, Blackwell Publishing Ltd, 2006, pp. 311–341.
- 33 S. Ito, K. Wakamatsu, M. d'Ischia, A. Napolitano and A. Pezzella, in *Melanins and Melanosomes: Biosynthesis, Biogenesis, Physiological, and Pathological Functions*, ed. J. Borovanský and P. A. Riley, Wiley-Blackwell, 2011, pp. 167–185.
- 34 H. Okuda, K. Wakamatsu, S. Ito and T. Sota, *J. Phys. Chem. A*, 2008, **112**, 11213–11222.
- 35 J. McGinness, P. Corry and P. Proctor, *Science*, 1974, **183**, 853–855.
- 36 E. D. Gowacki, M. Irimia-Vladu, S. Bauer and N. S. Sariciftci, *J. Mater. Chem. B*, 2013, **1**, 3742–3753.
- 37 A. B. Mostert, B. J. Powell, I. R. Gentle and P. Meredith, *Appl. Phys. Lett.*, 2012, **100**, 093701.
- 38 C. F. O. Graeff, G. B. Silva, F. Nüesch and L. Zuppiroli, *Eur. Phys. J. E: Soft Matter Biol. Phys.*, 2005, **18**, 21–28.
- 39 G. Saulis, R. Lap, R. Praneviit and D. Mickeviius, *Bioelectrochemistry*, 2005, **67**, 101–108.